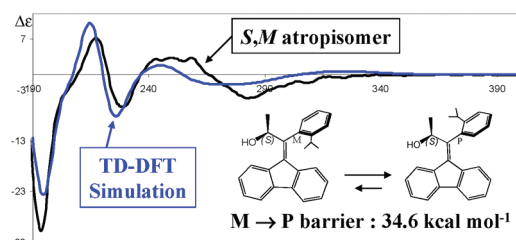


Structure, Conformation, Stereodynamics, and
Absolute Configuration of the Atropisomers
of Fluorenylidene DerivativesLodovico Lunazzi, Michele Mancinelli, and
Andrea Mazzanti*Department of Organic Chemistry "A. Mangini", University
of Bologna, Viale Risorgimento 4, Bologna 40136, Italy

mazzanti@ms.fci.unibo.it

Received November 25, 2010

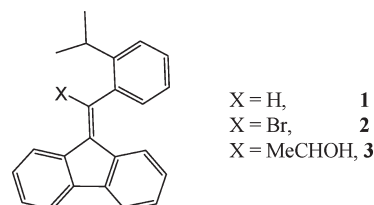


The barrier for the interconversion of the conformational atropisomers of an aryl fluorenylidene derivative was determined by variable-temperature NMR technique. In the case of a more hindered compound the two atropisomers were isolated and the structure determined by X-ray diffraction. The absolute configuration was assigned by theoretical interpretation of the Electronic Circular Dichroism spectrum (ECD).

Hindered derivatives of fluorenyl and of analogous derivatives have been synthesized and investigated as models for studying the so-called molecular motors.^{1–6} With the purpose of contributing to the comprehension of some of the related properties we synthesized the fluorenyl derivatives **1–3** (Scheme 1) and investigated their stereochemistry by means of dynamic NMR and ECD spectroscopy as well as by X-ray diffraction and DFT calculations.

The variable-temperature ¹³C spectrum of compound **1** (X = H) shows that the methyl signal broadens on cooling and eventually splits into a pair of equally intense lines at –106 °C (Figure 1). The line shape simulation provides a set of rate constants, corresponding to a free energy of activation (ΔG^\ddagger) of 8.9 kcal mol^{–1}. This feature indicates that the plane

SCHEME 1



of the isopropylphenyl ring is not coplanar with that of the fluorenylidene moiety. At low temperature the rotation about the bond joining these two planes is slow in the NMR time scale and in these conditions this bond corresponds to a stereogenic (chiral) axis. Consequently, the molecule displays an asymmetric conformation (C_1 point group) that entails the existence of two conformational enantiomers (atropisomers).⁷ such an asymmetry makes the isopropyl methyl groups diastereotopic, thus anisochronous.⁸ The measured ΔG^\ddagger value corresponds, therefore, to the rotation barrier required for the interconversion of the two atropisomers. Indeed DFT calculations⁹ show that the two mentioned planes are twisted by 54.7° (see Figure S-1 of the SI) and also indicate that in the transition state the two planes become essentially coplanar, with the isopropyl group pointing toward the ethylenic hydrogen. The energy computed for such a rotational transition state is 8.5 kcal mol^{–1} higher than the ground state, in good agreement with the experimental barrier.

When a bulkier substituent, like bromine, replaces the ethylenic hydrogen (compound **2**, X = Br) the ¹H NMR spectrum displays two diastereotopic methyl groups even at ambient temperature. These signals remain anisochronous also at higher temperatures (+120 °C), implying that the two atropisomers, generated by the chirality axis, could be configurationally stable. This is confirmed by the analysis on an enantioselective HPLC column, where compound **2** displays two separated lines for the two atropisomers (Figure S-2 in the SI). DFT calculations indicate that the transition state, having the isopropylphenyl coplanar with bromine (Figure S-3 of the SI), has an energy 29 kcal mol^{–1} higher than the ground state, when the isopropyl is pointing toward the bromine atom. This transition state shows, in addition, that the double bond is twisted by about 39°, in order to lower the steric clash between the ortho-hydrogen of the phenyl and the H-1 hydrogen of the fluorene ring.¹⁰ Such a theoretical

- (1) Feringa, B. L. *J. Org. Chem.* **2007**, 72, 6635–6652.
- (2) ter Wiel, M. K. J.; Feringa, B. L. *Tetrahedron* **2009**, 65, 4332–4339.
- (3) Geertsema, E. M.; van der Molen, S. J.; Martens, M.; Feringa, B. L. *Proc. Natl. Acad. Sci. U.S.A.* **2009**, 106, 16919–16924.
- (4) Kulago, H.; Mes, E. M.; Klok, M.; Meetsma, A.; Brouwer, A. M.; Feringa, B. L. *J. Org. Chem.* **2010**, 75, 666–679.
- (5) Pijper, T. C.; Pijper, D.; Pollard, M. M.; Dumur, F.; Davey, S. G.; Meetsma, A.; Feringa, B. L. *J. Org. Chem.* **2010**, 75, 825–838.
- (6) Chen, W.-C.; Lee, Y.-W.; Chen, C.-Y. *Org. Lett.* **2010**, 12, 1472–1475.

(7) Kuhn, R. *Molecular Asymmetry*. In *Stereochemie*; Freudenberg, K., Ed.; Franz Deuticke: Leipzig, 1933; pp 803–824. Oki, K. Recent Advances in Atropisomerism. In *Topics in Stereochemistry*; Allinger, N. L., Eliel, E. E., Wilen, S. H., Eds.; Wiley Interscience: New York, 1983; Vol. 14, pp 1–76. For a review on atropisomerism see: Bringmann, G.; Price Mortimer, A. J.; Keller, P. A.; Gresser, M. J.; Garner, J.; Breuning, M. *Angew. Chem., Int. Ed.* **2005**, 44, 5384–5427.

(8) Mislow, K.; Raban, M. *Top. Stereochem.* **1967**, 1, 1. Jennings, W. B. *Chem. Rev.* **1975**, 75, 307. Eliel, E. L. *J. Chem. Educ.* **1980**, 57, 52. Casarini, D.; Lunazzi, L.; Macciantelli, D. *J. Chem. Soc., Perkin Trans. 2* **1992**, 1363–1370.

(9) B3LYP/6-31G(d) level. *Gaussian 03*, Revision E.01, Frisch, M. J. et al.; Gaussian, Inc., Wallingford, CT, 2004. See the SI for the complete reference.

(10) In the alternative transition state where the isopropyl points away from the bromine the energy is even higher (38 kcal mol^{–1}) and the twisting angle of the double bond is about 50°.

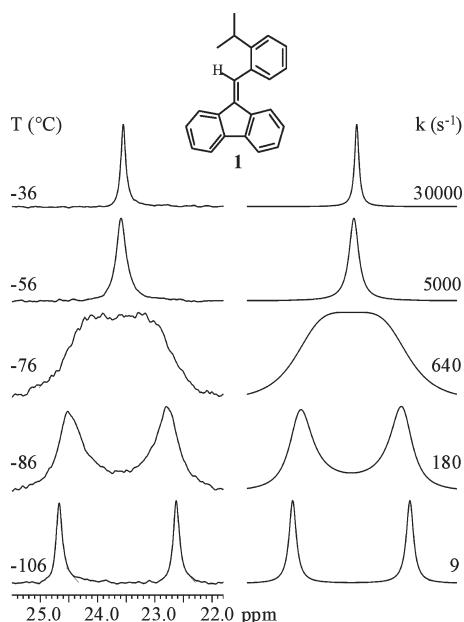


FIGURE 1. Temperature dependence of the ^{13}C methyl signal (150.8 MHz in CD_2Cl_2) of compound **1** (left) and line shape simulations (right) with the rate constants reported.

barrier accounts for the observed configurational stability of the atropisomers of **2**. However, we were unable to isolate the two atropisomers because of the very small chromatographic separation, despite the various attempts on a number of enantioselective columns. To achieve such a separation and to maintain a very high enantiomerization barrier, we prepared compound **3**, where the MeCHOH group is introduced in the place of bromine by reacting the lithiate of **2** with acetaldehyde. Compound **3** bears, in addition to the chirality axis, also a stereogenic carbon atom, so that two configurationally stable diastereoisomers are expected to occur. The synthetic procedure yields in fact two diastereoisomers, as revealed by the HPLC separation showing the signals of a major **3a** (80%) and of a minor **3b** (20%) compound as shown in the middle trace of Figure S-4 of the Supporting Information (first and second eluted, respectively). Each of these diastereoisomers is expected to exist as a pair of enantiomers due to the chirality axis and indeed when an enantioselective HPLC column is employed, four peaks are observed. The first and the second peak correspond to the two enantiomers of **3b**, the third and fourth peak correspond to the two enantiomers of **3a** (see Figure S-4 in the SI). X-ray diffraction of a single crystal of the second eluted enantiomer of the minor diastereoisomer **3b** provided the structure reported in Figure 2 (bottom, right). Although the absence of a sufficiently heavy atom prevented an unambiguous assignment of the absolute configuration by the anomalous dispersion method,¹¹ the S,M configuration reported in Figure 2 gives a fit of the experimental data (Flack parameter¹²) that is slightly better than that obtained by assuming the R,P configuration.

(11) Peerdeman, A. F.; van Bommel, A. J.; Bijvoet, J. M. *Nature* **1951**, *168*, 271–272. For a review on the use of X-ray Crystallography for the determination of the absolute configuration see: Flack, H. D.; Bernardinelli, G. *Chirality* **2008**, *20*, 681–690.

(12) Flack, H. D. *Acta Crystallogr.* **1983**, *A39*, 876–881.

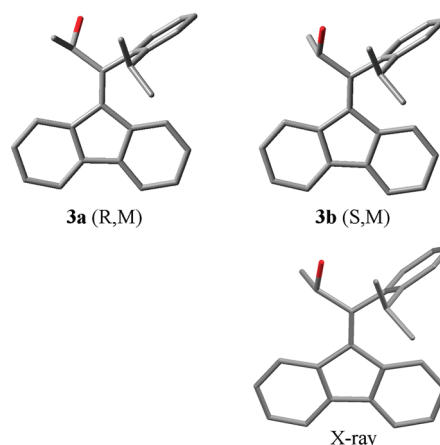


FIGURE 2. Top: DFT computed structure of the diastereoisomers **3a** and **3b** (in each case only one of the two possible enantiomers is displayed). Bottom: Experimental X-ray structure of **3b**.

To confirm this indication, we approached the determination of the absolute configuration of compound **3b** by making use of chiroptical techniques. In particular we simulated the Electronic Circular Dichroism spectra by TD-DFT calculations, because this technique has become highly reliable and it has been successfully employed to assign the absolute configuration of complex organic molecules.¹³

Starting from the geometry determined in the solid state, a conformational search was carried out by minimizing all the possible conformations obtainable by the 3-fold rotation of the MeCHOH group and of the OH group. All the conformations were optimized by using DFT at the B3LYP/6-31G(d) level, and the harmonic vibrational frequencies of each conformation were calculated at the same level to confirm their stability (no imaginary frequencies were observed), and to evaluate the free energy of each conformation by ZPE correction. After DFT minimization, in addition to the conformation of **3b** reported in Figure 2 (which corresponds to the global minimum), two other conformations were found to fall in a 2 kcal mol^{-1} range (see Figure S-5 in the SI). These three conformations were selected for the simulation of the ECD spectrum. Using the optimized geometries, the electronic excitation energies and rotational strengths were calculated by using TD-DFT at the BH&HLYP/6-311++G(d,p) level¹⁴ and assuming S,M absolute configuration. The results are shown in Figure S-6 of the SI (GS-1 to GS-3).¹⁵ The patterns of the three spectra are

(13) Mazzeo, G.; Giorgio, E.; Zanasi, R.; Berova, N.; Rosini, C. *J. Org. Chem.* **2010**, *75*, 4600–4603. Pescitelli, G.; Di Pietro, S.; Cardellicchio, C.; Annunziata, M.; Capozzi, M.; Di Bari, L. *J. Org. Chem.* **2010**, *75*, 1143–1154. Jacquemin, D.; Perpète, E. A.; Ciofini, I.; Adamo, C.; Valero, R.; Zhao, Y.; Truhlar, D. G. *J. Chem. Theory Comput.* **2010**, *6*, 2071–2085. Gioia, C.; Fini, F.; Mazzanti, A.; Bernardi, L.; Ricci, A. *J. Am. Chem. Soc.* **2009**, *131*, 9614–9615. Stephens, P. J.; Pan, J. J.; Devlin, F. J.; Cheeseman, J. R. *J. Nat. Prod.* **2008**, *71*, 285–288. For reviews see: Bringmann, G.; Bruhn, T.; Maksimenka, K.; Hemberger, Y. *Eur. J. Org. Chem.* **2009**, 2717–2727. Bringmann, G.; Gulder, T. A. M.; Reichert, M.; Gulder, T. *Chirality* **2008**, *20*, 628–642. Berova, N.; Di Bari, L.; Pescitelli, G. *Chem. Soc. Rev.* **2007**, *36*, 914.

(14) *Gaussian 09*, Revision A.01; Frisch, M. J. et al.; Gaussian, Inc., Wallingford, CT, 2009. See the SI for the complete reference. In *Gaussian 09* the BH&HLYP functional has the form: $0.5E_{\text{X}}^{\text{HF}} + 0.5E_{\text{X}}^{\text{LSDA}} + 0.5\Delta E_{\text{X}}^{\text{Becke88}} + E_{\text{C}}^{\text{LYP}}$. Becke, A. D. *J. Chem. Phys.* **1993**, *98*, 1372–77.

(15) The rotational strengths were calculated in the length and velocity representations. The resulting values are very similar, and the errors due to basis set incompleteness are therefore very small, or negligible. See: Stephens, P. J.; McCann, D. M.; Devlin, F. J.; Cheeseman, J. R.; Frisch, M. J. *J. Am. Chem. Soc.* **2004**, *126*, 7514–7521.

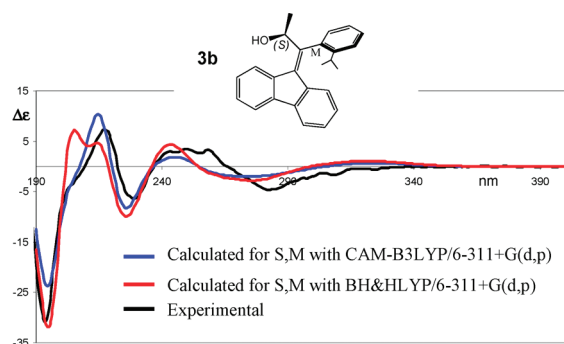


FIGURE 3. Experimental ECD spectrum (black trace) of the second eluted atropisomer of the minor diastereoisomer **3b** and TD-DFT computed traces (red and blue) obtained assuming the absolute SM configuration.

different, in particular between the spectrum calculated for the lowest energy ground state and the other two. For this reason the shape of the final simulated spectrum could be strongly influenced by errors in the evaluation of the relative populations of the conformations. However, the best calculated geometry corresponds to the experimental structure observed in the solid state. The same calculations were repeated by using a different model (CAM-B3LYP¹⁶) in order to check the solidity of the theoretical approach (Figure S-6 of the SI, bottom).¹⁷ The final simulated ECD spectra shown in Figure 3 were obtained taking into account the 78:18:4 ratio derived from Boltzmann distribution based on the ZPE corrected energy values of the three conformers of **3b**. The theoretical simulations obtained by the TD-DFT approach employing two different functionals^{13,17} show that the experimental trace is reproduced quite satisfactorily by assuming the S,M configuration: consequently the absolute configuration of the other (first eluted) atropisomer of **3b** must be R,P.

The computed DFT structure of **3b** (Figure 2, top right) is very close to that experimentally determined by X-ray, so that the computed structure for **3a** (Figure 2, left) can be likewise considered a satisfactory representation of the major diastereoisomer.¹⁸ In addition, the ECD spectrum of the second eluted enantiomer of the major diastereoisomer **3a** was theoretically reproduced following the same procedure reported above,⁹ by assuming the S,P configuration (Figures S-7 and S-8 of the SI). It also should be stressed that the computed energy for the diastereoisomer **3b** is lower by 1.8 kcal mol⁻¹ than that of **3a**, whereas the proportion of the latter (80%) was found much higher than that of **3b** (20%) in the reaction mixture. This apparent discrepancy could be due to the fact that the reaction to produce **3** is under kinetic rather than thermodynamic control. Indeed the Li intermediate required to produce **3** by low-temperature reaction with CH₃CHO has a computed rotation barrier around the Ar–CLi bond equal to 12.6 kcal mol⁻¹. This implies that, at the temperature of the formation of the lithiate (–85 °C), the corresponding lifetime of the rotamer is quite long (about

100 s). This suggests that CH₃CHO (which is added only a few seconds after the formation of the Li intermediate) reacts with the Li intermediate when the latter is in a locked conformation (see Figure S-9 of the SI). This feature might account for the occurrence of the mentioned diastereoselectivity.

As the measurement of the free energy barrier of the diastereoisomers **3a** and **3b** is inaccessible to the dynamic NMR technique, a kinetic approach was used. When a DMSO/D₂O (10:1 v/v) solution of the isolated diastereoisomer **3a** (which is computed to be the least stable) is kept at +135 °C, the interconversion into **3b** begins to take place until the thermodynamic equilibrium is reached, whereby the **3b/3a** ratio becomes 62:38, as opposed to the kinetic ratio **3b/3a** = 20:80. This proves that the diastereoisomer **3b** is the thermodynamically more stable species, as predicted by calculations. The kinetic path of this process was followed by monitoring the variation of the NMR signal ratio as a function of the time (see Figure S-10 of the SI) and the free energy of activation for the **3b** into **3a** interconversion was found equal to 34.6 kcal mol⁻¹ (at +135 °C).

The energy for the corresponding rotation transition state (Figure S-11 of the SI) was computed to be 32.8 kcal mol⁻¹ higher than that of the ground state of **3b**.¹⁹

The calculated barrier is lower than the measured Gibbs free energy barrier (34.6 kcal). This could be due to a negative entropy of activation for the rotational process due to restricted freedom of the proximate isopropyl and MeCHOH groups in the rotational transition state TS-1.²⁰

Experimental Section

9-(2-Isopropylbenzylidene)-9H-fluorene (1)²¹. To an oven-dried round-bottomed flask were added 1.00 g (6.02 mmol) of fluorene and 1.86 g of *t*-BuOK (16.54 mmol), followed by 50 mL of THF. The reaction was heated to reflux with vigorous stirring, then 2-isopropylbenzaldehyde was added (1.07 g, 7.22 mmol), and the reaction was allowed to reflux overnight. After cooling to room temperature, the reaction mixture was poured into a large excess of 1 M HCl and crushed ice, and it was extracted with Et₂O. The organic layer was washed with brine and dried over Na₂SO₄. After removal of the Et₂O the crude was purified by silica chromatography with hexanes/Et₂O 10/1 v/v. Analytical samples were obtained by semipreparative HPLC chromatography (Phenomenex Luna C8, 250 × 10 mm, eluent CH₃CN/H₂O 90:10 v/v, 5 mL/min). ¹H NMR (600 MHz, CD₂Cl₂, 25 °C, δ 5.32): δ 1.21 (6H, d, *J* = 7.00 Hz), 3.23 (1H, septet, *J* = 7.0 Hz), 6.98–7.04 (2H, m), 7.25–7.32 (2H, m), 7.35–7.48 (5H, m), 7.73 (1H, d, *J* = 7.6 Hz), 7.76 (1H, d, *J* = 7.4 Hz), 7.84 (1H, s), 7.87 (1H, d, *J* = 7.4 Hz). ¹³C NMR (150.8 MHz, CD₂Cl₂, 25 °C, δ 53.8): δ 23.6 (2 CH₃), 31.3_s (CH), 119.9_s (CH), 120.0 (CH), 120.7 (CH), 125.0 (CH), 125.7 (CH), 126.2 (CH), 127.0 (CH), 127.3 (CH), 127.4 (CH), 128.5 (CH), 128.7 (CH), 128.9 (CH), 129.9 (CH), 135.8 (q), 137.2 (q), 137.3 (q), 139.5 (q), 139.6 (q).

(19) In the alternative transition state where the isopropyl points away from the MeCHOH group the energy is even higher (45.6 kcal mol⁻¹).

(20) An alternative conversion path between the two diastereoisomers might correspond to a dehydration process of the secondary alcohol to alkene, where the rotation of the phenyl moiety could take place with a lower barrier, followed by rehydration. In this case, however, the presence of a large molar excess of D₂O in the NMR sample should lead to a partial (or total) deuteration of the CH and Me groups, a feature that it is not experimentally observed. This confirms that the energy barrier determined is that of the rotation of the aryl group.

(21) Dane, E. L.; Maly, T.; Debelouchina, G. T.; Griffin, R. G.; Swager, T. M. *Org. Lett.* **2009**, *11*, 1871–1874.

(16) Yanai, T.; Tew, D.; Handy, N. *Chem. Phys. Lett.* **2004**, *393*, 51–57.

(17) The use of more than one model enhances the reliability of the method, and it can serve as an evaluation of the amplitude of the possible error. See: Check, C. E.; Gilbert, T. M. *J. Org. Chem.* **2005**, *70*, 9828–9834.

(18) Neither of the enantiomers of the major diastereoisomer **3a** yielded crystals suitable for a structural determination by X-ray diffraction.

141.3 (q), 147.7 (q). HRMS(EI): m/z calcd for $C_{23}H_{20}$ 296.15650, found 296.15611.

9-(Bromo(2-isopropylphenyl)methylene)-9H-fluorene (2). To an oven-dried round-bottomed flask was added 1.17 g of 9-(2-isopropylbenzylidene)-9H-fluorene (3.95 mmol, in 30 mL of glacial acetic acid). The resulting suspension was heated to reflux and additional acetic acid was added dropwise until a homogeneous solution was formed. The mixture was cooled to room temperature and a slight excess of a bromine solution (4.75 mmol, 0.47 M in acetic acid) was added dropwise over 5 min. The resulting red solution was allowed to stir overnight at room temperature until a white precipitate formed. Then NaOH (0.158 g 3.95 mmol) and absolute ethanol (25 mL) were added. The reaction was refluxed for 60 min and then cooled to room temperature. The solution was acidified with 0.5 M HCl and extracted with Et_2O . The organic layer was then washed with brine and dried over Na_2SO_4 . After removal of the Et_2O the material was purified by silica chromatography with hexanes/ Et_2O 10:1 v/v. Analytical samples were obtained by semipreparative HPLC chromatography (Phenomenex Luna C8, 250 \times 10 mm, eluent CH_3CN/H_2O 90:10 v/v, 5 mL/min). 1H NMR (600 MHz, CD_3CN , 25 $^\circ C$, δ 1.95): δ 1.00 (3H, d, J = 7.0 Hz), 1.28 (3H, d, J = 7.0 Hz), 3.17 (1H, septet, J = 7.0 Hz), 6.02 (1H, d, J = 7.9 Hz), 6.86–6.89 (1H, m), 7.26–7.32 (2H, m), 7.36–7.40 (1H, m), 7.46 (1H, dt, J = 1.2, 7.8 Hz), 7.50–7.58 (3H, m), 7.76 (1H, d, J = 7.5 Hz), 7.85 (1H, d, J = 7.5 Hz), 8.89 (1H, d, J = 7.9 Hz). ^{13}C NMR (150.8 MHz, CD_3CN , 25 $^\circ C$, δ 117.5): δ 23.1 (CH_3), 23.4 (CH_3), 30.6 (CH), 119.8 (CH), 120.1 (CH), 124.5 (q), 124.8 (CH), 126.2 (CH), 127.1 (CH), 127.2 (CH), 127.3 (CH), 127.5 (CH), 128.2 (CH), 128.8 (CH), 129.7 (CH), 130.3 (CH), 136.4 (q), 137.6 (q), 138.1 (q), 139.8 (q), 140.9 (q), 141.3 (q), 146.1 (q). HRMS(EI): m/z calcd for $C_{23}H_{19}Br$ 374.06701, found 374.06736.

1-(9H-fluoren-9-ylidene)-1-(2-isopropylphenyl)propan-2-ol (3a and 3b). To an oven-dried round-bottomed flask was added 100 mg of 9-(bromo(2-isopropylphenyl)methylene)-9H-fluorene (0.266 mmol, in 20 mL of dry THF). The mixture was cooled to $-85^\circ C$ and $n-BuLi$ (0.18 mL, 0.29 mmol, 1.6 M in hexane, 1.1 equiv) was added dropwise. The solution became immediately red, and after 1 min, 0.03 mL of acetaldehyde (neat, 0.53 mmol) was added, yielding an almost colorless solution. The mixture was then warmed to room temperature and the reaction was quenched with H_2O and extracted with Et_2O . The organic layer was washed with brine and dried over Na_2SO_4 . After removal of the Et_2O the crude was purified by silica chromatography with hexanes/ Et_2O 10:1 v/v. The resulting mixture of the two diastereoisomers **3a** and **3b** was separated by semipreparative HPLC chromatography (Phenomenex Synergy Polar-RP 4 μm , 250 \times 21.2 mm, eluent CH_3CN/H_2O 90:10 v/v, 20 mL/min). Separation of the two enantiomers of **3a** and **3b** was obtained by semipreparative HPLC on an enantioselective column (Daicel Chiralcel AD-H 5 μm , 250 mm \times 21.2 mm, eluent hexane/ $iPrOH$ 95:5 v/v, 20 mL/min). **3a** (1 $^\circ$ eluted): 1H NMR (600 MHz, $CDCl_3$, 25 $^\circ C$, TMS): δ 0.86 (3H, d, J = 6.7 Hz), 1.24 (3H, d, J = 7.0 Hz), 1.46 (3H, d, J = 6.7 Hz), 1.80 (1H, d, J = 5.5 Hz), 2.90 (1H, septet, J = 6.7 Hz), 5.79 (1H, quintet, J = 5.5 Hz), 5.85 (1H, d, J = 7.9 Hz), 6.79–6.83 (1H, m), 7.15–7.21 (2H, m),

7.31–7.34 (1H, m), 7.37–7.43 (2H, m), 7.48–7.49 (2H, m), 7.64 (1H, d, J = 7.3 Hz), 7.76–7.77 (1H, m), 8.01 (1H, d, J = 7.6 Hz). ^{13}C NMR (150.8 MHz, $CDCl_3$, 25 $^\circ C$, TMS): δ 21.8 (CH_3), 24.4 (CH_3), 25.0 (CH_3), 31.2 (CH), 67.7 (CH), 119.2 (CH), 119.9 (CH), 125.9 (CH), 126.4 (CH), 126.6 (CH), 126.9 (2 CH), 127.5 (CH), 127.9 (CH), 128.3 (CH), 128.9 (CH), 129.5 (CH), 135.1 (Cq), 136.5 (Cq), 137.0 (Cq), 138.8 (Cq), 140.2 (Cq), 141.3 (Cq), 147.0 (Cq), 147.2 (Cq). HRMS(EI): m/z calcd for $C_{25}H_{24}O$: 340.18272, found 340.18244.

3b (2 $^\circ$ eluted): 1H NMR (600 MHz, CD_3CN , 25 $^\circ C$, 1.95 ppm): δ 0.81 (3H, d, J = 6.7 Hz), 1.22 (3H, d, J = 7.0 Hz), 1.52 (3H, d, J = 6.7 Hz), 2.88 (1H, d, J = 6.2 Hz), 3.03 (1H, septet, J = 6.7 Hz), 5.79 (1H, d, J = 8.1 Hz), 5.82 (1H, quintet, J = 6.6 Hz), 6.79 (1H, t, J = 7.5 Hz), 7.11 (1H, d, J = 7.9 Hz), 7.19 (1H, t, J = 7.3 Hz), 7.30–7.33 (1H, m), 7.40–7.45 (2H, m), 7.48–7.53 (2H, m), 7.73 (1H, d, J = 7.3 Hz), 7.83–7.86 (1H, m Hz), 7.96–7.98 (1H, m). ^{13}C NMR (150.8 MHz, CD_3CN , 25 $^\circ C$, 117.5 ppm): δ 22.5 (CH_3), 23.2 (CH_3), 24.0 (CH_3), 31.6 (CH), 66.8 (CH), 119.3 (CH), 119.9 (CH), 125.5 (CH), 126.22 (CH), 126.23 (CH), 126.61 (CH), 126.63 (CH), 127.6 (CH), 127.7 (CH), 128.1 (CH), 128.5 (CH), 128.53 (CH), 132.3 (Cq), 137.2 (Cq), 137.5 (Cq), 138.8 (Cq), 140.0 (Cq), 140.7 (Cq), 148.1 (Cq), 151.2 (Cq). HRMS(EI): m/z calcd for $C_{25}H_{24}O$ 340.18272, found 340.18239.

ECD Spectra. Standard UV absorption spectra were recorded at 25 $^\circ C$ in acetonitrile on the racemic mixtures, in the 200–400 nm spectral region. Maximum molar absorption coefficients were recorded at 193 nm for **3b** (ϵ = 59 300) and 193 nm for **3a** (ϵ = 54 400). ECD spectra were recorded at 24 $^\circ C$ in acetonitrile solutions (5×10^{-5} M), using a path length of 0.2 cm. Spectra were recorded in the range 180–400 nm; reported $\Delta\epsilon$ values are expressed as $L \text{ mol}^{-1} \text{ cm}^{-1}$.

NMR Spectroscopy. NMR spectra were obtained at 600 MHz for 1H and at 150.8 MHz for ^{13}C . The assignments of the 1H and ^{13}C signals were obtained by bidimensional experiments (edited-gHSQC and gHMBC sequences). The variable-temperature spectra were recorded at 600 MHz for 1H and 150.8 MHz for ^{13}C ; temperature calibration and line shape simulation methods were described elsewhere.²²

Acknowledgment. The authors received financial support from the University of Bologna (RFO) and from MIUR, Rome (PRIN national project “Stereoselection in Organic Synthesis, Methodologies and Applications”).

Supporting Information Available: DFT computed ground states and transition states structures for **1**, **2**, **3a**, and **3b**; enantioselective HPLC traces for compounds **2**, **3a**, and **3b**; computed components of the ECD spectrum of **3a** and **3b**, TD-DFT simulation of the ECD spectrum of **3a**, kinetics of the thermal equilibration of **3a**, crystallographic data of **3b**, and 1H , ^{13}C NMR spectra and computational data of **1–3**. This material is available free of charge via the Internet at <http://pubs.acs.org>.

(22) For a recent review see: Casarini, D.; Lunazzi, L.; Mazzanti, A. *Eur. J. Org. Chem.* **2010**, 2035–2056.